

ELECTRONS RF AUTO-FOCUSING AND CAPTURE IN BUNCHERS

D.Tronc, A.Setty
 General Electric CGR MeV, BP 34, 78530 Buc, France

Summary

We gradually evolved during these last years to new design guidelines of focusing by the RF field alone. The new 3D code PARDYN follows in time, the most complicated electron trajectories with relativistic space-charge effects. We apply it to the FRASCATI and to the SATURNE / OXFORD-IBM bunchers. Experimental results are given. Beams with very small cross sections are obtained.

Introduction

Classical bunchers insure only longitudinal phase stability. However in the special case of electrons submitted to a strong accelerating field, the incompatibility principle stated by McMillan (1) does not apply. RF field components can ensure simultaneously radial and longitudinal stability by an unconventional choice for the geometry of several cells in X-band (2), of two cells in S-band (3-5), of the input region of the first cell at lower frequency (6). Radial behaviour can be analyzed by noting optical effects at the input and output regions of the cells. The equivalent lenses have either a convergent, a divergent or a null effect. It depends on the electron beam to RF electrical field dephasing. Their positions can be modified as long as overall longitudinal acceleration occurs.

RF auto-focusing

We analyze S band solutions. The frequency domain near 3 GHz offers the greatest opportunities as the dephasing law along the buncher and the field shape in the first cell acts with comparable weights. We gradually evolved from the classical approach in three stages.

First we understood how radial control was possible by choosing a greater than usual length for the first cell : bunched electrons cross its output region when the field amplitude is nearly zero and radial defocusing does not occur. Analysis were given in (3). Application was made to ORION compact medical linacs in 1983. However the price paid for this radial control is a poor capture ratio as the late electrons are lost (the cell is too long for them).

The second stage uses a moderate field level in this first long cell, together with a rather large gun voltage. Then all the electrons cross the cell thanks to their initial energy but cannot go backward to the gun if they have lost all their kinetic energy. Application was made to the FRASCATI buncher design in 1985 (4). However the price paid for this good capture is the relatively high gun voltage required.

In the third stage we optimized the shape of the electrical field in the first cell and not only its average level (5). A low field "mesa" prebunches and preaccelerates (fig.1). Then the field increases to a peak and accelerates the nascent bucket. In practice one can only approximate this ideal field law by proper choice of an asymmetrical cell geometry. The required gun voltage is lowered as well as the

unavoidable radial dispersion at the input due to the initially very different electron phases. Afterwards the position of the input part of the second strongly accelerating cell insures a complementary RF focusing.

These refinements are possible when cells have reduced holes on-axis giving a precise localisation of the equivalent lenses (three such lenses are indicated for locally null dephasing on fig.1). They were applied in 1987 to the buncher common to the SATURNE medical linacs and to the OXFORD-IBM light source injector.

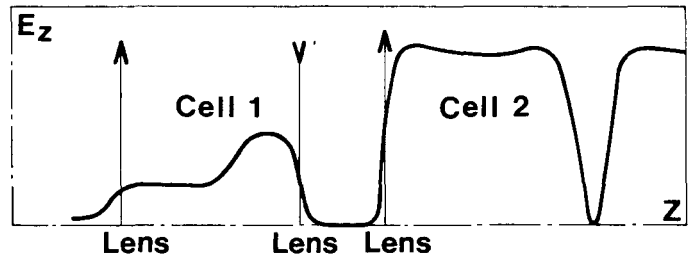


Figure 1. Accelerating field law for electrons RF auto-focusing and capture.

Simulation code

The electron dynamics are complicated. Their energies varies from zero to more than one MeV in a length comparable to the prebucket dimension. Velocities are different at the same abscissa. On-axis oscillations occur. Space-charge effect can locally be large. RF asymmetrical field phase and amplitude laws must be shaped precisely.

Such non-linear bunching and acceleration process requires a step-by-step simulation made in time. All efforts have been made to implement it as an highly interactive fully three-dimensional tool for design purposes.

PARDYN includes backward as well as forward movements and relativistic space-charge effects. The provided elements are: RF accelerating cell, drift, magnetic lens, quadrupole, dipole and bending magnet. The accelerating cell may include a magnetic lens and a dipole. Subharmonic frequencies can be used.

ORION buncher (stage 1)

Figure 2 shows a photograph of the hole made by the 5 MeV beam on the X-rays target surface. Initially an (unwanted) thin layer of copper covered the tungsten. The impact region is well seen as this layer has melted. The magnification is 100 and the uncovered surface is .65 mm X .50 mm. The microbunch cross section is lower as microbunches do not superimpose exactly (accelerating field level and other parameters varies) and as melting occurs outside the impact. Other measurements indicate a microbunch cross section of .35 mm X .20 mm ! This occurs at a moderate .3 m distance from the gun. The cathode diameter is 8 mm. There is no focusing other than the RF one.

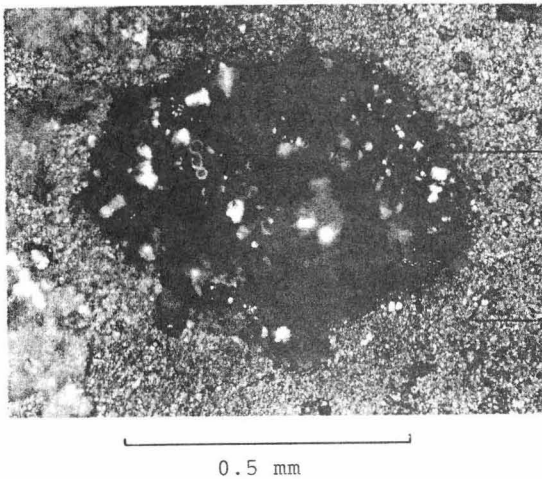


Figure 2. Beam impact on X-rays target.

FRASCATI buncher (stage 2)

It was delivered in December 1986 to LNF. Unfortunately independent measurements with beam were not made on this part before its installation as head of the multisections linac. Beam controls at the buncher exit were made in July 1988. They were limited in scope as in precision, due to the short distance available between buncher and first section, and due to a tight planning.

We summarize our estimates (7) which differs from the LNF ones (8) as follows : The beam energy is 20 ± 1 MeV. The current inside 5 mm diameter is 40 % and inside 15 mm is 80 %. In this last case, the measured capture ratio lie somewhere between 35 % and 50 %.

We have made simulations to define more precisely the accelerated bunch dimensions in the last buncher cell (9). Initial conditions are a gun current of 5A with a pessimistic emittance of 180 pi mm mrad at 90 keV and for a 7 mm diameter. Figure 3 shows the longitudinal phase histogram. 50% of the electrons lie inside 15° , 63% inside 30° and 82% inside 50° . Such non linear distribution is well known.

Figure 4 shows the radial extension. 67% of the electrons lie inside 3 mm diameter, 85 % inside 5 mm. The lower measured value of 50 % can be attributed to the beam divergence which occurs at the end of the RF field, to the windows and to some off-axis beam position. Figure 5 is a "photograph" of the microbunch. It has an assymmetric longitudinal density with a "comet" shape.

We summarize these simulations as follows : for 5A delivered by the gun, two-third of the 2.5A accelerated are in the 30° forward part of a "comet" shaped bunch OR inside a 3 mm radius. We estimate that half the accelerated electrons, or 1.25A lies simultaneously inside 30 degrees and 3 mm diameter.

SATURNE/OXFORD-IBM buncher (stage 3)

Measurements made without any magnetic focusing on the latest SATURNE medical section gives an estimated beam cross section at 25 MeV and at 3 m from the gun of less than $1 \text{ mm} \times 1 \text{ mm}$ (10). Two-third of the gun current is captured. Simulations give an increase greater than 5 in density over previous stage 1 design. We illustrate them at mid-acceleration point, around 10 MeV and after 1 m. Figure 6 gives the longitudinal phase histogram. Figure 7 gives the radial distribution. Figure 8 gives the energy distribution. The bunch characteristics are such that for 300 mA delivered by the gun and 200 mA accelerated, 130 mA lies inside a 1 % energy band width, a 10 degrees phase extension and a 2.4 mm diameter.

Conclusion

We feel that the dynamics of the "well-grown" electrons are understood and that the three available parameters (cell lengths or phase law, relative field cell amplitudes and shape of the field in a cell) have been properly optimized. We will look closely to electrons which after a complicated behaviour are lost. They create stray X-rays (a major problem in radiotherapy) and increase the beam loading.

References

- (1) H.G. Hereward, "The general theory of linear accelerators" in *Linear Accelerators* edited by P.M.Lapostolle and A.L.Septier, 1970.
- (2) R.H. Miller and al., "RF phase focusing in portable X-band linear accelerators", 1985 Part.Acc.Conf., IEEE-NS32, 3231.
- (3) D.Tronc, "Electron injector computer simulations", Europhysics Conf., Berlin, 1983, Springer, Lectures notes in Physics, no 215, page 231; D.Tronc and al., "Electron injector designs.", 1985 Part.Acc.Conf., IEEE-NS32, 3246.
- (4) D.Tronc and al., "Design of a high intensity electron buncher", 1986 Linear Acc.Conf., Stanford, 472.
- (5) D.Tronc, French patent 88 04707.
- (6) J.Aucouturier and H.Leboutet, French patent 83 08427.
- (7) D.Tronc, A.Setty, "Measurements made on the Frascati SW injector...", GE-CGR MeV, DT.13908, July 1988.
- (8) C.Biscari and al., "Design of a prebuncher system...", LNF Frascati, July 1988.
- (9) D.Tronc, "Dynamique du groupeur de Frascati et Grenoble", GE-CGR MeV, DT.14074, August 1988.
- (10) C.Perraudin and F.Dugardin, GE-CGR MeV, private communications.

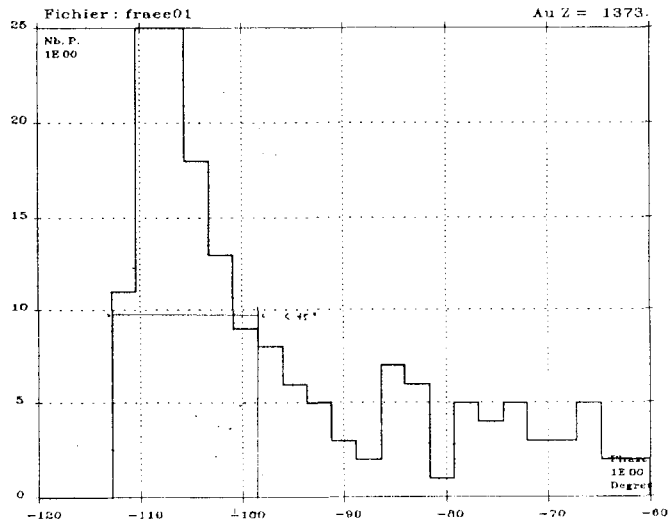


Figure 3. Longitudinal phase histogram (Frascati buncher)

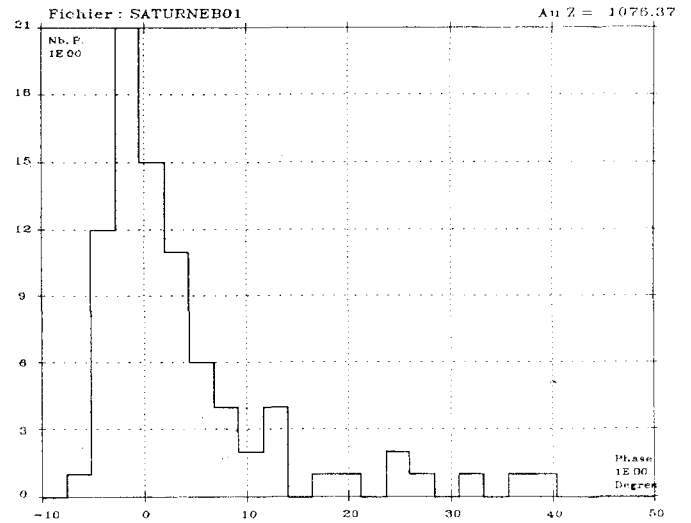


Figure 6. Longitudinal phase histogram (Saturne/Oxford-IBM buncher)

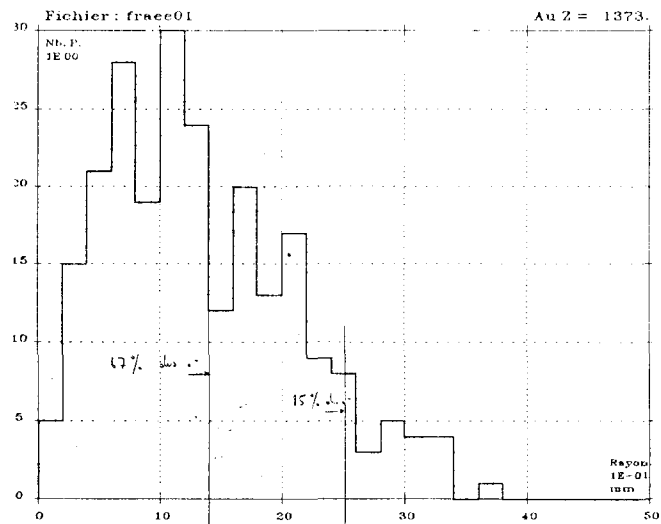


Figure 4. Radial extension (Frascati buncher)

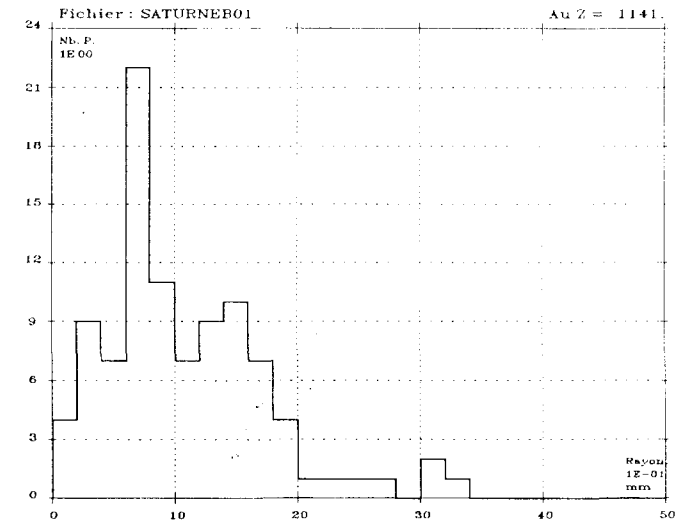


Figure 7. Radial extension (Saturne/Oxford-IBM buncher)

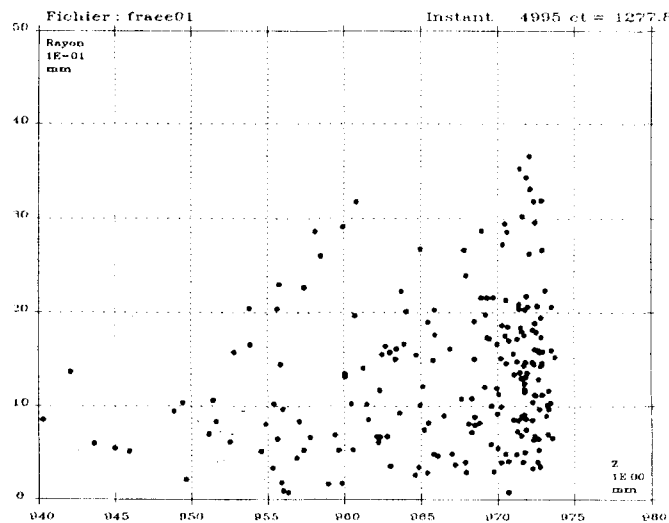


Figure 5. Side-view of a microbunch (Frascati buncher)

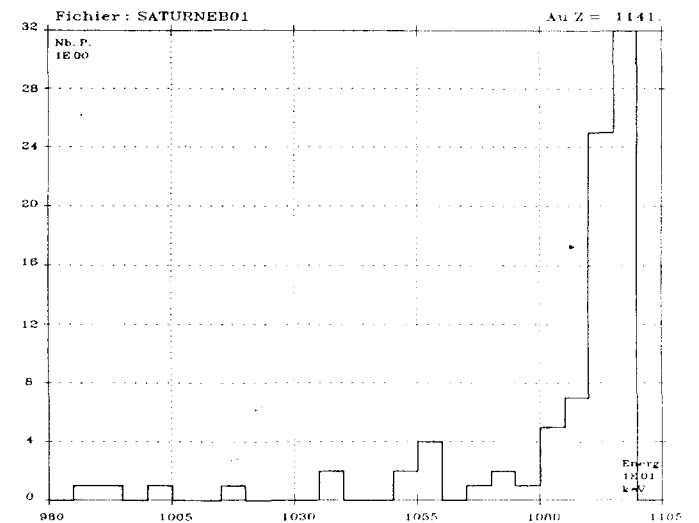


Figure 8. Energy histogram (Saturne/Oxford-IBM buncher)